

Synthesis of Pt/GO composite as an electrochemical sensor for determination of synthetic corticosteroid triamcinolone as doping agents in sports

Ziyi Wang^{1,*}, Yumang Zhang²

¹ Harbin Sport University, Harbin, 150026, China

² College of Life Science, Changchun Sci-Tech University, Changchun, 130600, China

*E-mail: wangziyi041128@sina.com

Received: 5 April 2022 / Accepted: 16 May 2022 / Published: 6 June 2022

The hydrothermal production of Pt/GO nanocomposite as an electrochemical sensor for determining triamcinolone (TA) as a doping agent in urine samples was presented in this study. The creation of a well-crystallized Pt/GO nanocomposite was confirmed by FE-SEM and XRD studies, which revealed well-dispersed Pt nanoparticles with a spherical shape that were adorned on GO nanosheets. The results of electrochemical characterization using DPV and amperometry techniques revealed that the Pt/GO/GCE displayed stable and selective electrocatalytic attractive in the TA reduction reaction, with sensing parameters of sensitivity, detection limit, and linear range calculated as 0.08099 $\mu\text{A}/\text{M}$, 12 nM, and 1 to 130 μM , respectively. When the performance of the proposed electrochemical TA sensor was compared to that of other previously reported TA electrochemical sensors, it was discovered that the proposed sensor exhibited a wider linear range of Pt/GO/GCE than other sensors. In prepared genuine samples from human urine samples originating from four patients aged 22 to 33 years undergoing pharmacological treatment with TA, the reliability and usefulness of Pt/GO/GCE to determine TA were studied. The acquired RSD values (less than 4.14%) and the good agreement between the amperometric and ELISA assays indicated that the developed amperometric TA sensor had sufficient detection precision and reliability for determining TA in human urine samples.

Keywords: Electrochemical sensor; Triamcinolone; Human urine samples; Pt/GO nanocomposite

1. INTRODUCTION

Triamcinolone (TA; (1S,2S,4R,8S,9S,11S,12R,13S)-12-fluoro-11-hydroxy-8-(2-hydroxyacetyl)-6,6,9,13-tetramethyl-5,7-dioxapentacyclo[10.8.0.0^{2,9}.0^{4,8}.0^{13,18}]icosa-14,17-dien-16-one) is a muscle-building corticosteroid [1]. Corticosteroids are synthetic counterparts of testosterone [2, 3]. TA, as a glucocorticoid medication, also suppresses the release of inflammatory chemicals in the body [4-6]. The itching, redness, dryness, crusting, scaling, inflammation, and pain of numerous skin disorders

such as allergic reactions, eczema, and psoriasis are treated with TA topically [7, 8]. Certain forms of cancer are also treated with TA [9-12]. Upset stomach, stomach irritation, vomiting, headache, dizziness, sleeplessness, restlessness, depression, anxiety, acne, increased hair growth, easy bruising, and irregular or nonexistent menstrual periods are all possible side effects of TA [13-15]. In 2014, the World Anti-Doping Agency added TA to its forbidden list because it helps athletes shed weight without causing a major reduction in power. When injected orally, intravenously, intramuscularly, or rectally, TA is illegal in competition [16, 17]. As a result, identifying and determining the level of TA in clinical samples and biological fluids of patients and athletes is critical, particularly for those on high-dose antibiotic therapy [18-21].

High-performance liquid chromatography (HPLC) [22, 23], UV derivative spectrophotometry and spectrodensitometry [24-26], chemical ionization mass spectrometry [27], gas chromatography [28], and electrochemical methods [29-34]. Electrochemical methods have been shown to have high selectivity and sensitivity for TA measurement in clinical samples when compared to other analytical methods. To the best of our knowledge, not only are there few studies on improving the stability of TA electrochemical sensors, but there are also few studies on electrochemical TA determination, which are indicated to require more study for improved sensitivity, linear range response and stability of electrochemical TA for application in clinical samples [29-32]. This research focused on the simple synthesis of the Pt/GO nanocomposite and its development as a highly stable, wide linear range and sensitive electrochemical sensor for the detection of TA as doping agents in urine samples.

2. EXPERIMENT

2.1. Synthesis Pt/GO nanocomposite

A Pt/GO nanocomposite was prepared using a hydrothermal method [35]. 0.5 g of GO (99%, Luoyang Tongrun Info Technology Co., Ltd., China) was ultrasonically dispersed in 10 mL of solution containing 20 mg of $\text{H}_2\text{PtCl}_6 \cdot 6\text{H}_2\text{O}$ (99%, Luoyang Tongrun Info Technology Co., Ltd., China) aqueous solution. The mixture was magnetically stirred for 15 minutes. For hydrothermal reaction of the Pt ions, the mixture was transferred into a Teflon-sealed autoclave at 95 °C for 3 hours. After cooling, the product was collected by centrifugation, and washed with deionized water and ethanol several times. Before modification of GCE, it was first polished with alumina slurry (<5 μm , 99.5%, Sigma-Aldrich) to establish a mirror surface. Then, using a magnetic stirrer, 1.0 mg/mL of dispersed Pt/GO nanocomposite was prepared, and 10 L of Pt/GO suspension was dropped on the GCE and dried for 20 minutes under an infrared light, followed by electrochemical reduction for 2 minutes in 0.1 M phosphate buffer solutions (PBS, pH 7.4) [36].

2.2. Preparation of real samples of urine

Four athletes, aged 22 to 33, supplied urine samples after taking Tricort pills, which contain 4 mg of TA per tablet. Because the half-life of TA is believed to be 10–30 hours [29], urine samples

were collected after 10 hours of tablet administration. The samples were centrifuged at 1000 rpm for 10 minutes, and used to prepare 0.1 M PBS pH 7.4 as real samples for electrochemical analyses. The TA enzyme-linked immunosorbent assay kit (ELISA, NEOGEN Co., USA) was also employed for the determination of the TA level in urine samples.

2.3. Characterizations

Crystallographic and morphological analyses were carried out using an X-ray diffractometer (XRD) and field emission scanning electron microscopy (FE-SEM), respectively. Electrochemical measurements were performed using differential pulse voltammetry (DPV) and amperometry techniques in an Autolab PGSTAT100 potentiostat–galvanostat controlled by a GPES 4.9 software (Ecochemie, The Netherlands). The potentiostat–galvanostat had a three-electrode electrochemical cell with a Pt plate, Ag/AgCl, and modified GCE as the counter, reference, and working electrodes, respectively. 0.1 M phosphate buffer solution (PBS) with pH 7.4 was used as an electrolyte which was prepared by mixing stock solutions of 0.1 M NaCl (99%, Sigma-Aldrich), and 0.1 M NaH₂PO₄–Na₂HPO₄ (99%, Sigma-Aldrich).

3. RESULTS AND DISCUSSION

3.1. Structural characterization

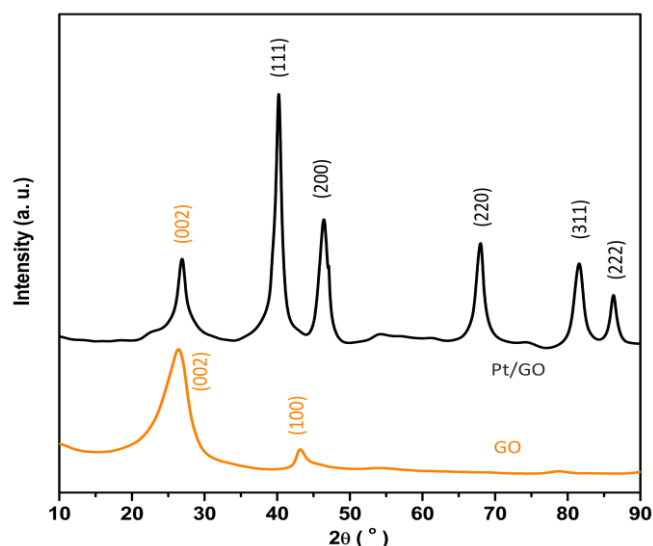


Figure 1. The XRD patterns of GO and Pt/GO nanocomposite.

Figure 1 shows the XRD patterns of GO and Pt/GO nanocomposite. There are two diffraction peaks at 26.55° and 43.11° on the XRD pattern of GO, which are ascribed to the (002) and (100) planes of graphite from GO (JCPDS Card no. 01-0646) [37-39]. Pt/GO nanocomposite XRD patterns exhibit distinctive peaks at 39.97°, 46.55°, 68.05°, 88.44°, and 86.41°, which are indexed to the (111),

(200), (220), and (311) planes, respectively, which detect the fcc phase of Pt (JCPDS Card 04-0783) [40, 41]. Furthermore, the XRD pattern of Pt/GO shows an extra diffraction peak corresponding to GO's (002) reflection, suggesting that GO is present on the Pt nanostructure.

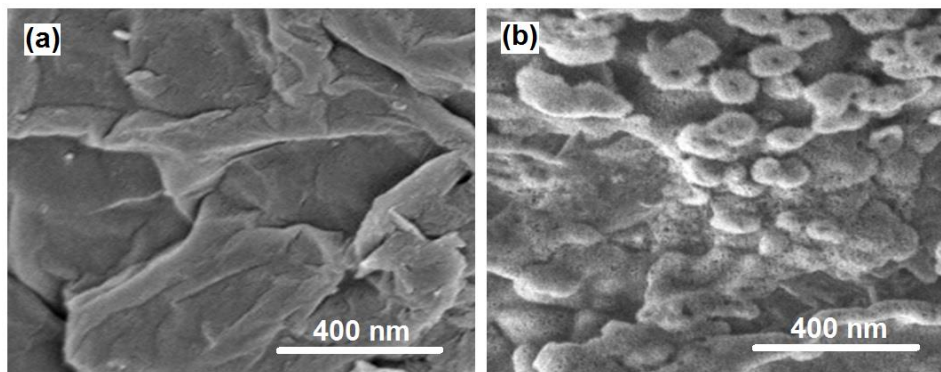


Figure 2. FE-SEM images of (a) GO nanosheets, (b) Pt/GO nanocomposite.

FE-SEM images from Figure 2 display the morphology of GO and Pt/GO nanocomposite. As observed from the FE-SEM image of GO, GO morphology shows a two-dimensional structure of layered and wrinkled nanosheets with several folds. FE-SEM images of Pt/GO show the well-dispersed Pt nanoparticles with spherical shapes that are decorated on GO nanosheets, indicating that Pt nanoparticles and GO are well combined [42]. The average diameter of anchored Pt nanoparticles is about 80nm. These results confirm the formation of the Pt/GO nanocomposite. The nanocomposite of Pt/GO provides large specific surface areas with numerous active sites which can absorb more analytes [43-46]. Furthermore, the obtained high porosity allows charges to easily transit inside the interior pore channels, enhancing electrocatalytic activity.

3.2. Electrochemical characterization

At a scan rate of 15 mV/s, Figure 3 shows the electrochemical responses of bare and GO and Pt/GO nanocomposite modified GCE 0.1 M PBS with pH 7.4 containing 100 μ M TA. In the DPV curves of bare GCE, there is no visible redox peak, as seen. However, at potentials of -0.93 V and -0.91 V, respectively, GO/GCE and Pt/GO/GCE show a cathodic peak, which is due to catalytic reduction of the α,β unsaturated carbonyl function of TA [31, 47, 48]. The cathodic peak for Pt/GO/GCE is detected at a lower potential, and its current is approximately 2 times that of GO/GCE. It demonstrates that Pt/GO/GCE exhibits significant electrocatalytic attractiveness in the reduction of TA, which could be attributed to the fact that Pt nanoparticles coated on GO nanosheets increase the effective area, resulting in fast electron transport [49-52]. GO serves as a mediator to facilitate electron transfer [53-55]. According to FE-SEM findings, the linked structure of dispersed Pt nanoparticles on GO nanosheets efficiently prevents graphene and nanoparticle agglomeration in nanocomposed

structures, increases specific area, and improves catalytic effectiveness [56-58]. Moreover, Pt nanoparticles as a recognized catalyst can improve the rate of chemical reaction [57, 59], and the anchoring of Pt nanoparticles on oxygen-containing groups of GO nanosheets accelerates electron transport and electrochemical reaction and also possibly improves the performance of catalyst [60-62]. Thus, synergistic effect of Pt nanoparticles decorated GO nanosheets to boost electrocatalytic signal [56, 63].

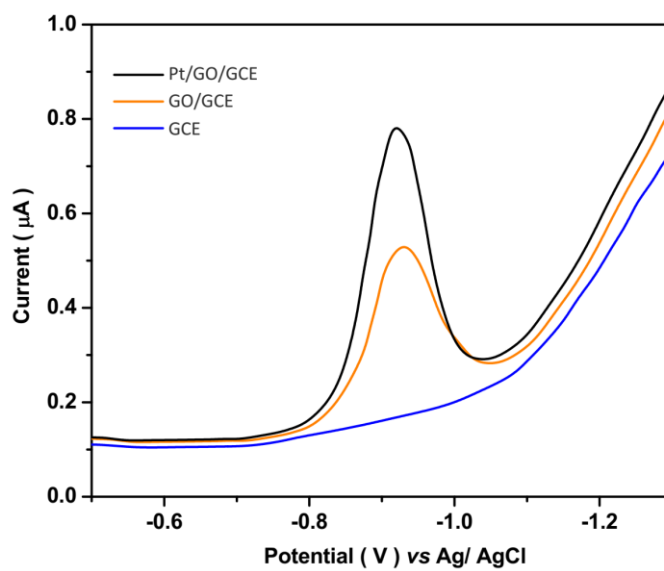


Figure 3. DPV curves of bare and GO and Pt/GO nanocomposite modified GCE 0.1 M PBS with pH 7.4 containing 100 μ M TA at a scan rate of 15 mV/s.

Figure 4 shows the results of testing the stability of GO/GCE and Pt/GO/GCE electrochemical responses in an electrochemical cell containing 0.1 M PBS with pH 7.4 in the presence of 100 M TA at a scan rate of 15 mV/s across 150 sweeps in the potential range of 0.5 V to -1.3 V. As shown in Figure 4, the initial and 150th recorded DPV curves of GO/GCE and Pt/GO/GCE shows 9% and 2% decrease, respectively, indicating to more stable signal of Pt/GO/GCE due to high chemical stability of Pt nanoparticle, and the successful electropolymerization of MIPs that mainly depends on the stability and strength of the monomer and binding interactions between the Pt nanoparticles and strong interaction between Pt and abundant π sites in graphitized carbon of graphene nanosheets during hydrothermal reaction [64, 65]. Therefore, Pt/GO nanocomposite modified GCE was selected as a favorable catalyst for the electrochemical sensing of TA [66-68].

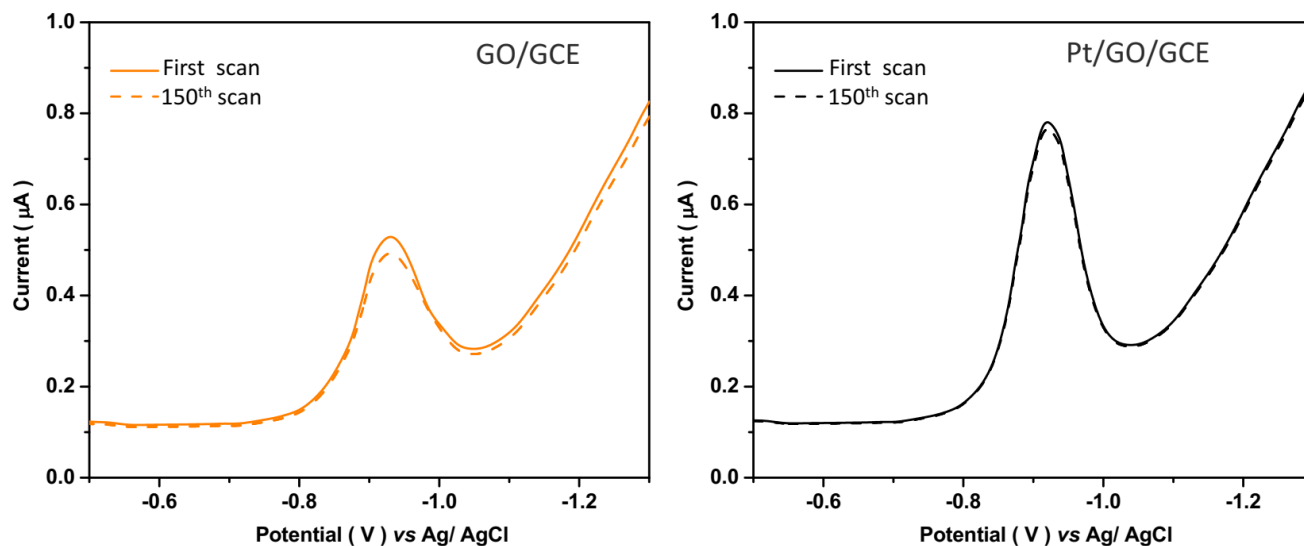


Figure 4. The initial and 150th recorded DPV curves of GO/GCE and Pt/GO/GCE in electrochemical cell containing 0.1 M PBS with pH 7.4 in presence 100 μ M TA at a scan rate of 15 mV/s under successive 150 sweeps in the potential range from -0.5 V to -1.3 V.

The amperometric observations and accompanying calibration graph of Pt/GO/GCE response current to serial injections of 10 μ M TA at a potential of -0.91 V in 0.1 M PBS with pH 7.4 are shown in Figure 5. Pt/GO/GCE exhibits a rapid response to the addition of TA solution, signaling a fast electron transfer on the surface of Pt/GO, which could be linked to the porous nanocomposite matrix and simple desorption of reaction intermediates, as well as high porosity [69, 70].

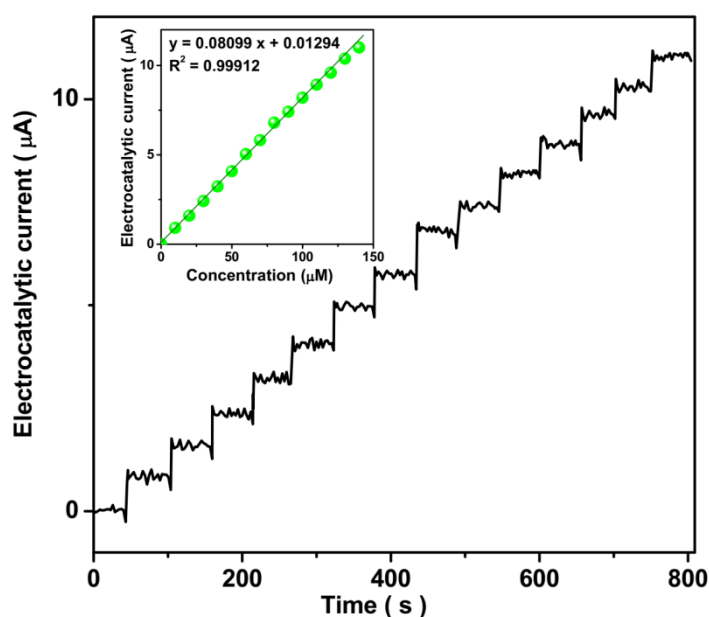


Figure 5. Amperometric measurements and corresponding calibration graph of response current of Pt/GO/GCE to successive additions of 10 μ M TA at potential of -0.91 V in 0.1 M PBS with pH 7.4.

The amperometric signal is linearly raised with consecutive additions of 10 μM TA solution from 1 to 130 M, as shown in the calibration graph, and the sensing parameters of sensitivity and detection limit are computed as 0.08099 $\mu\text{A}/\mu\text{M}$ and 12 nM, respectively. Table 1 compares the performance of the proposed electrochemical TA sensor to that of other TA electrochemical sensors published in the literature. It has been discovered that Pt/GO/GCE has a wider linear range than other sensors, indicating that the suggested sensor outperforms previously reported sensors. This is attributed to the increased electron conductivity of the Pt/GO nanocomposite and the synergistic catalytic action between Pt and GO [71-75]. The consecutive reaction between the Pt nanoparticles and oxygen-containing functional groups of GO can help to release the Pt crystal lattice and promote the activity of the catalysis [76-78].

Table 1. Comparison between the performance of proposed electrochemical TA sensor in this study and other reported TA electrochemical sensors in the literatures.

Electrodes	Technique	Detection limit (nM)	Linear range (μM)	Ref.
Pt/GO/GCE	Amperometry	12	1 to 130	This study
SWNTs/EPPGE	DPV	0.89	10^{-4} to 0.025	[29]
CPE	CV	150	2 to 46	[32]
GCE	DPSV	254	0.5 to 127	[31]
GCE	SWSV	25.4	0.038 to 127	[31]
Hanging mercury drop electrode	ACSV	0.3	10^{-3} to 0.09	[30]

EPPGE: Edge plane pyrolytic graphite electrode; CPE: Carbon Paste Electrode, CV: Cyclic voltammetry; DPSV: Differential pulse stripping voltammetry; SWSV: square wave stripping voltammetry; ACSV: Adsorptive cathodic stripping voltammetry

Using amperometric experiments of Pt/GO/GCE under successive additions of 10 μM TA and 6-fold interfering compounds at a potential of -0.91 V in 0.1 M PBS with pH 7.4, the impact of various substances as potential interfering compounds from pharmaceuticals and/or in biological fluids on the determination of TA was evaluated. Figure 6 shows the electrocatalytic currents obtained for all compounds at a potential of -0.91 V, showing that there is no response to the addition of interfering chemicals and a strong electrocatalytic signal to the addition of TA in the electrochemical cell. Therefore, there is no substantial interference effect for the determination of TA in presence of presented substances in Figure 6, and the proposed electrochemical TA sensor can show good selectivity for the determination of TA in pharmaceuticals and/or in biological fluid samples [79-81].

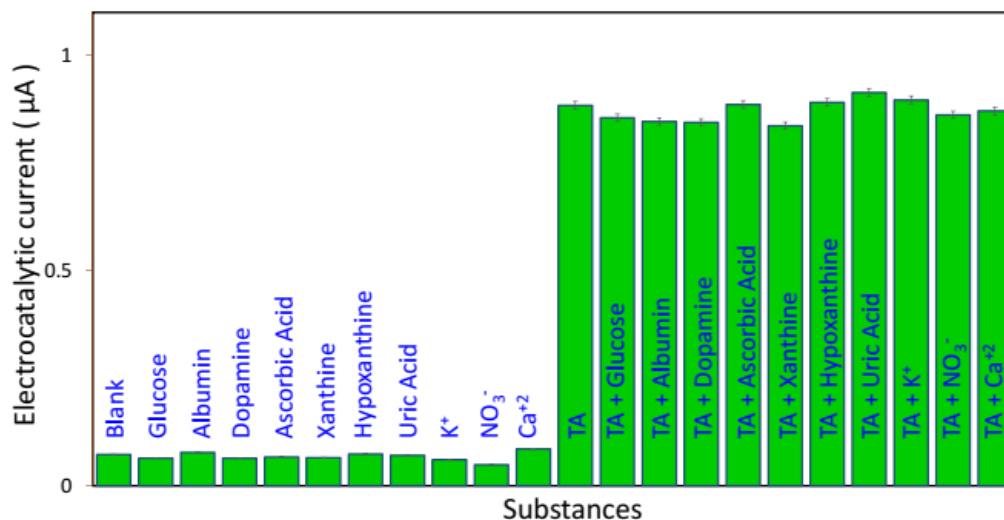


Figure 6. The results of amperometric electrocatalytic currents of Pt/GO/GCE under successive additions of 10 μM TA and 6-fold interfering compounds at potential of -0.91 V in 0.1 M PBS with pH 7.4; (blank sample is referred to the 0.1 M PBS without any analyte)

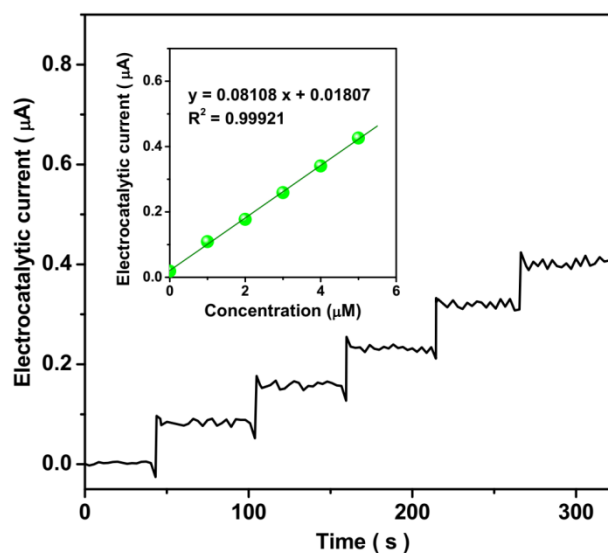


Figure 7. Amperometric measurements and corresponding calibration graph of response current of Pt/GO/GCE to successive additions of 10 μM TA at potential of -0.91 V in 0.1 M PBS with pH 7.4 prepared from urine sample of first patient.

In prepared genuine samples from human urine samples originating from four athletes undergoing pharmaceutical therapy with TA, the reliability and usability of Pt/GO/GCE for determining TA were studied. Using Pt/GO/GCE at -0.91 V and serial injections of TA solution, amperometric measurements were used to evaluate the TA level in produced 0.1M PBS from urine samples. The amperometry data and corresponding calibration plot from the first patient sample (S1) are shown in Figure 7, revealing that the TA content in the processed sample is 0.221 μM , which is

extremely near to the TA level found by the ELISA assay (Table 2). The amperometric and ELISA assays were also performed for the other three urine samples and the findings of an average of five times of both of assays for the determination of TA are summarized in Table 2, implying good agreement between the two assays. In addition, the obtained RSD values are presented in Table 2 which is less than 4.14%, indicating the developed amperometric TA sensor has acceptable detection precision, and reliability for determination of TA in human urine samples.

Table 3. The findings of ELISA and amperometry assays to determination of TA in prepared real samples from athlete urine samples originating from four patients undergoing pharmacological treatment with TA

Sample	Content of TA in prepared urine samples (μM)			
	Amperometry		TA ELISA kit	
	Pt/GO/GCE	RSD (%)	ELISA	RSD (%)
S1	0.221	± 3.22	0.228	± 3.61
S2	0.151	± 3.29	0.155	± 4.09
S3	0.194	± 4.14	0.196	± 4.04
S4	0.166	± 4.09	0.170	± 3.77

4. CONCLUSION

This research focused on the development of a Pt/GO nanocomposite as an electrochemical sensor for the detection of TA as doping agents in urine samples. The hydrothermal technique was used to make the Pt/GO nanocomposite. The development of a well-crystallized Pt/GO nanocomposite was revealed by structural characterizations, which revealed well-dispersed Pt nanoparticles with a spherical shape that were adorned on GO nanosheets. The electrochemical characterization revealed that Pt/GO/GCE exhibited steady and selective electrocatalytic attractiveness in the TA reduction reaction, with sensing parameters of sensitivity, detection limit, and linear range of $0.08099 \mu\text{A}/\mu\text{M}$, 12 nM, and 1 to 130 μM , respectively. When the performance of the proposed electrochemical TA sensor was compared to that of other reported TA electrochemical sensors, it was discovered that it demonstrated a wider linear range of Pt/GO/GCE than other sensors, which was attributed to the improved electron conductivity of the Pt/GO nanocomposite and the synergistic catalytic effect of Pt and GO. The simultaneous reaction of Pt nanoparticles with oxygen-containing functional groups of GO can aid in the liberation of the Pt crystal lattice and increase catalytic activity. In prepared genuine samples from human urine samples originating from four patients aged 22 to 33 years undergoing pharmacological therapy with TA, the reliability and usefulness of Pt/GO/GCE to determine TA were studied. The developed amperometric TA sensor demonstrated acceptable detection precision and reliability for determining TA in human urine samples, according to the findings.

References

1. B. Ivković, M. Crevar, A. Cvetanović, K. Ubavkić and B. Marković, *Acta Chromatographica*, 1 (2022) 1.
2. H. Maleh, M. Alizadeh, F. Karimi, M. Baghayeri, L. Fu, J. Rouhi, C. Karaman, O. Karaman and R. Boukherroub, *Chemosphere*, (2021) 132928.
3. L. Nan, C. Yalan, L. Jixiang, O. Dujuan, D. Wenhui, J. Rouhi and M. Mustapha, *RSC Advances*, 10 (2020) 27923.
4. W.-F. Lai, R. Tang and W.-T. Wong, *Pharmaceutics*, 12 (2020) 725.
5. R. Mohamed, J. Rouhi, M.F. Malek and A.S. Ismail, *International Journal of Electrochemical Science*, 11 (2016) 2197.
6. T.-H. Zha, O. Castillo, H. Jahanshahi, A. Yusuf, M.O. Alassafi, F.E. Alsaadi and Y.-M. Chu, *Applied and Computational Mathematics*, 20 (2021)
7. D.J. McCarty, *Arthritis & Rheumatism: Official Journal of the American College of Rheumatology*, 15 (1972) 157.
8. D. Jia, C. Li, Y. Zhang, M. Yang, X. Zhang, R. Li and H. Ji, *The International Journal of Advanced Manufacturing Technology*, 100 (2019) 457.
9. J.-G. Kim, S.O. Bae and K.S. Seo, *Supportive Care in Cancer*, 23 (2015) 2305.
10. X. Wang, C. Li, Y. Zhang, W. Ding, M. Yang, T. Gao, H. Cao, X. Xu, D. Wang and Z. Said, *Journal of Manufacturing Processes*, 59 (2020) 76.
11. A. Roghani, *AIMS Public Health*, 8 (2021) 655.
12. T.-H. Zhao, M.-K. Wang, G.-J. Hai and Y.-M. Chu, *Revista de la Real Academia de Ciencias Exactas, Físicas y Naturales. Serie A. Matemáticas*, 116 (2022) 1.
13. C. Xin, L. Changhe, D. Wenfeng, C. Yun, M. Cong, X. Xuefeng, L. Bo, W. Dazhong, H.N. LI and Y. ZHANG, *Chinese Journal of Aeronautics*, (2021) 1.
14. H. Karimi-Maleh, R. Darabi, M. Shabani-Nooshabadi, M. Baghayeri, F. Karimi, J. Rouhi, M. Alizadeh, O. Karaman, Y. Vasseghian and C. Karaman, *Food and Chemical Toxicology*, 162 (2022) 112907.
15. M. Nazeer, F. Hussain, M.I. Khan, E.R. El-Zahar, Y.-M. Chu and M. Malik, *Applied Mathematics and Computation*, 420 (2022) 126868.
16. Y. Zhang, H.N. Li, C. Li, C. Huang, H.M. Ali, X. Xu, C. Mao, W. Ding, X. Cui and M. Yang, *Friction*, 10 (2022) 803.
17. C. Liu and J. Rouhi, *RSC Advances*, 11 (2021) 9933.
18. C. Li, J. Li, S. Wang and Q. Zhang, *Advances in Mechanical Engineering*, 5 (2013) 986984.
19. N. Naderi, M. Hashim, J. Rouhi and H. Mahmodi, *Materials science in semiconductor processing*, 16 (2013) 542.
20. R.S. Moghadam, M. Akbari, Y. Alizadeh, A. Medghalchi and R. Dalvandi, *Middle East African Journal of Ophthalmology*, 26 (2019) 11.
21. Y.-M. Chu, B. Shankaralingappa, B. Gireesha, F. Alzahrani, M.I. Khan and S.U. Khan, *Applied Mathematics and Computation*, 419 (2022) 126883.
22. S. Sudsakorn, L. Kaplan and D.A. Williams, *Journal of pharmaceutical and biomedical analysis*, 40 (2006) 1273.
23. L. Chen, Y. Huang, X. Yu, J. Lu, W. Jia, J. Song, L. Liu, Y. Wang, Y. Huang and J. Xie, *Frontiers in pharmacology*, 12 (2021) 363.
24. Y.S. El-Saharty, N.Y. Hassan and F.H. Metwally, *Journal of pharmaceutical and biomedical analysis*, 28 (2002) 569.
25. J. Rouhi, S. Mahmud, S. Hutagalung and S. Kakooei, *Micro & Nano Letters*, 7 (2012) 325.
26. T.H. Zhao, M.I. Khan and Y.M. Chu, *Mathematical Methods in the Applied Sciences*, (2021) 1.
27. D. Courtheyn, J. Vercammen, M. Logghe, H. Seghers, K. De Wasch and H. De Brabander, *Analyst*, 123 (1998) 2409.

28. G. Rodchenkov, V. Uralets, V. Semenov and P. Leclercq, *Journal of High Resolution Chromatography*, 11 (1988) 283.
29. R.N. Goyal, V.K. Gupta and S. Chatterjee, *Biosensors and Bioelectronics*, 24 (2009) 3562.
30. E. Hammam, *Chemia Analytyczna*, 52 (2007) 43.
31. C. Vedhi, R. Eswar, H.G. Prabu and P. Manisankar, *International Journal of Electrochemical Science*, 3 (2008) 509.
32. P. Zagrzewski, K. Belikov and I. Zinchenko, *Methods*, 13 (2018) 136.
33. H. Karimi-Maleh, C. Karaman, O. Karaman, F. Karimi, Y. Vasseghian, L. Fu, M. Baghayeri, J. Rouhi, P. Senthil Kumar and P.-L. Show, *Journal of Nanostructure in Chemistry*, (2022) 1.
34. H.-H. Chu, T.-H. Zhao and Y.-M. Chu, *Mathematica Slovaca*, 70 (2020) 1097.
35. H. Li and X. Cui, *International journal of hydrogen energy*, 39 (2014) 19877.
36. K. Yasuda, A. Taniguchi, T. Akita, T. Ioroi and Z. Siroma, *Physical Chemistry Chemical Physics*, 8 (2006) 746.
37. M.-L. Chen, C.-Y. Park, J.-G. Choi and W.-C. Oh, *Journal of the Korean Ceramic Society*, 48 (2011) 147.
38. S.M.M. Dezfouli and S. Khosravi, *Pakistan Journal of Medical & Health Sciences*, 14 (2020) 1236.
39. T.-H. Zhao, Z.-Y. He and Y.-M. Chu, *AIMS Mathematics*, 5 (2020) 6479.
40. Y. Karatas, E. Kuyuldar, H. Acidereli, M. Gulcan and F. Sen, *Scientific Reports*, 9 (2019) 18553.
41. M. Liu, C. Li, Y. Zhang, Q. An, M. Yang, T. Gao, C. Mao, B. Liu, H. Cao and X. Xu, *Frontiers of Mechanical Engineering*, 16 (2021) 649.
42. E. Ashpazzadeh, Y.-M. Chu, M.S. Hashemi, M. Moharrami and M. Inc, *Applied Mathematics and Computation*, 427 (2022) 127171.
43. Q. He, Y. Wu, Y. Tian, G. Li, J. Liu, P. Deng and D. Chen, *Nanomaterials*, 9 (2019) 115.
44. F. Chahshouri, H. Savaloni, E. Khani and R. Savari, *Journal of Micromechanics and Microengineering*, 30 (2020) 075001.
45. H. Savaloni, E. Khani, R. Savari, F. Chahshouri and F. Placido, *Applied Physics A*, 127 (2021) 1.
46. T.-H. Zhao, B.-C. Zhou, M.-K. Wang and Y.-M. Chu, *Journal of Inequalities and Applications*, 2019 (2019) 1.
47. H.S. de Boer, W. Van Oort and P. Zuman, *Analytica Chimica Acta*, 120 (1980) 31.
48. J.W. Honour, *Hormone Assays in Biological Fluids*, 1 (2006)
49. S. Lee, Y.J. Lee, J.H. Kim and G.-J. Lee, *Chemosensors*, 8 (2020) 63.
50. H. Savaloni, R. Savari and S. Abbasi, *Current Applied Physics*, 18 (2018) 869.
51. R. Savari, H. Savaloni, S. Abbasi and F. Placido, *Sensors and Actuators B: Chemical*, 266 (2018) 620.
52. Y. Chu and T. Zhao, *Mathematical Inequalities & Applications*, 19 (2016) 589.
53. G. Bharath, E. Alhseinat, R. Madhu, S.M. Mugo, S. Alwasel and A.H. Harrath, *Journal of Alloys and Compounds*, 750 (2018) 819.
54. R. Savari, J. Rouhi, O. Fakhar, S. Kakooei, D. Pourzadeh, O. Jahanbakhsh and S. Shojaei, *Ceramics International*, 47 (2021)
55. S.M.M. Dezfouli and S. Khosravi, *Indian Journal of Forensic Medicine and Toxicology*, 15 (2021) 2674.
56. Z. Xia, J. Fang, X. Zhang, L. Fan, A.J. Barlow, T. Lin, S. Wang, G.G. Wallace, G. Sun and X. Wang, *Applied Catalysis B: Environmental*, 245 (2019) 389.
57. Y. Ma, Q. Wang, Y. Miao, Y. Lin and R. Li, *Applied Surface Science*, 450 (2018) 413.
58. M.-K. Wang, M.-Y. Hong, Y.-F. Xu, Z.-H. Shen and Y.-M. Chu, *Journal of Mathematical Inequalities*, 14 (2020) 1.

59. H. Karimi-Maleh, H. Beitollahi, P.S. Kumar, S. Tajik, P.M. Jahani, F. Karimi, C. Karaman, Y. Vasseghian, M. Baghayeri and J. Rouhi, *Food and Chemical Toxicology*, (2022) 112961.
60. Y. Xin, J.-g. Liu, Y. Zhou, W. Liu, J. Gao, Y. Xie, Y. Yin and Z. Zou, *Journal of Power Sources*, 196 (2011) 1012.
61. H.K. Ebrahimi, S. Sohrabi, S. Jafarnejad, S. Iranmanesh and S. Esmaeilian, *Systematic Reviews in Pharmacy*, 11 (2020) 899.
62. S. Rashid, S. Sultana, Y. Karaca, A. Khalid and Y.-M. Chu, *Fractals*, 30 (2022) 2240026.
63. J. Rouhi, S. Mahmud, S.D. Hutagalung and S. Kakooei, *Journal of Micro/Nanolithography, MEMS, and MOEMS*, 10 (2011) 043002.
64. J. Tang, T. Wang, X. Sun, Y. Guo, H. Xue, H. Guo, M. Liu, X. Zhang and J. He, *Microporous and mesoporous materials*, 177 (2013) 105.
65. S. Jafarnejad, I. Mehrabi, M. Rezai and H.K. Ebrahimi, *Pakistan Journal of Medical and Health Sciences*, 14 (2020) 1412.
66. M.D. Bedrin, R.M. Putko and J.F. Dickens, *Sports Medicine and Arthroscopy Review*, 29 (2021) e71.
67. S.N. Hajiseyedazizi, M.E. Samei, J. Alzabut and Y.-m. Chu, *Open Mathematics*, 19 (2021) 1378.
68. S.A. Iqbal, M.G. Hafez, Y.-M. Chu and C. Park, *Journal of Applied Analysis & Computation*, 12 (2022) 770.
69. K.-J. Chen, K.C. Pillai, J. Rick, C.-J. Pan, S.-H. Wang, C.-C. Liu and B.-J. Hwang, *Biosensors and Bioelectronics*, 33 (2012) 120.
70. H.K. Ebrahimi, M. Amirmohamadi, S. Esmaeilian, S. Sohrabi, S. Iranmanesh, Z. Sohrabi and S. Jafarnejad, *Pakistan Journal of Medical and Health Sciences*, 14 (2020) 1426.
71. Z. Savari, S. Soltanian, A. Noorbakhsh, A. Salimi, M. Najafi and P. Servati, *Sensors and Actuators B: Chemical*, 176 (2013) 335.
72. Y. Liu, P. She, J. Gong, W. Wu, S. Xu, J. Li, K. Zhao and A. Deng, *Sensors and Actuators B: Chemical*, 221 (2015) 1542.
73. H. Ebrahimi, S. Jafarnejad, S. Sohrabi, A. Abbasi and S. Esmaeilian, *Journal of Critical Reviews*, 7 (2020) 685.
74. F. Jin, Z.-S. Qian, Y.-M. Chu and M. ur Rahman, *Journal of Applied Analysis & Computation*, 12 (2022) 790.
75. F. Wang, M.N. Khan, I. Ahmad, H. Ahmad, H. Abu-Zinadah and Y.-M. Chu, *Fractals*, 30 (2022) 2240051.
76. J. Rouhi, S. Mahmud, S.D. Hutagalung and N. Naderi, *Electronics letters*, 48 (2012) 712.
77. A.K. Karakka Kal, T.K. Karatt, J. Nalakath, M.B. Subhahar, S.A. Koshy, Z. Perwad and M.A. MP, *Analytical Science Advances*, 2 (2021) 427.
78. S.-Y. Chen, M. Fang, Y.-T. Lin, C.-F. Tsai, H.-F. Cheng and D.-Y. Wang, *Steroids*, 165 (2021) 108739.
79. K.A. Zahidah, S. Kakooei, M. Kermanioryani, H. Mohebbi, M.C. Ismail and P.B. Raja, *International Journal of Engineering and Technology Innovation*, 7 (2017) 243.
80. R. Ventura, P. Daley-Yates, I. Mazzoni, K. Collomp, M. Saugy, F. Buttgereit, O. Rabin and M. Stuart, *British Journal of Sports Medicine*, 55 (2021) 631.
81. F. Moreira, H. Carmo, P. Guedes de Pinho and M.d.L. Bastos, *Drug Testing and Analysis*, 13 (2021) 474.